MINERALOGIA POLONICA
Vol. 11, No 2 - 1980

Leonard KULIG[x], *Henryk TOMASZEWSKI*[x], *Jędrzej TORUŃ*[x]

MICROSCOPIC STUDIES OF THE INTERGRANULAR PHASE IN CORUNDUM MATERIALS

UKD 666.764.32:535.827.2:539.215.3:549.517.1+549.731.11:546.621+546.46

A b s t r a c t. A selected corundum material was investigated by TEM, SEM and EMPA methods. Two kinds of intergranular phase were found to be present: besides vitreous phase, microareas of aluminium-magnesium spinel were observed.

INTRODUCTION

The technology of production of corundum materials requires that precisely contolled amounts of admixtures be introduced into aluminium oxide in order to modify the properties of the resulting sinter.

Several investigators /Pampuch 1962, Kitajgorodski 1959,Burke 1960/ are of the opinion that these admixtures form a separate liquid phase with the participation of aluminium oxide being sintered. This phase, appearing at room temperature as an amorphous component, is commonly referred to as vitreous or intergranular phase. In view of the lower viscosity of liquid layers compared with the least ordered layers at the intergranular boundaries, the cited authors believe that the rearrangement of aluminium oxide grains in the presence of liquid proceeds more readily and at lower temperatures than in the solid phase. Accordingly, the process of rearrangement of grains is initiated the moment the liquid phase appears. The effect of liquid on the sintering process has already been noted at a liquid phase content of 0.01 - 0.5 mole %, and it has been found that the increase in its content does not produce any further significant changes.

[x]Institute of Technology of Electronic Materials, Warszawa, ul. Konstruktorska 6.

The positive effect of the liquid phase on the sintering process can be expected only if the solid phase is adequately wetted, which usually is the case in ceramic materials. The presence of the intergranular phase in corundum materials is also advantageous from the point of view of their future applications. According to the studies of Cole and Sommer /1961/ and Włosiński /1976/, the migration of this phase to the metallic layer is one of the factors responsible for the strength of the ceramics-to-metal seal. The morphology of the intergranular phase solidified in the cooling process also depends on the degree of wetting of the solid phase by liquid phase. When the wetting is adequate, the intergranular phase areas are represented in plane sections by more or less elongated forms of polygons, commonly by triangles.

Microscopic studies have revealed that the microareas of this phase, forming in the process of sintering, are some micrometres in size. Therefore, selective X-ray investigations of their chemical composition and structure are unsatisfactory, especially when their volume fractions are small. Using TEM, SEM and EMPA methods, it is possible to investigate the morphology, structure and chemical composition of the intergranular phase in selected microareas.

Since there is a certain divergence in opinions regarding the structure of the intergranular phase in corundum materials, microscopic studies of a chosen material were taken up at the ITEM.

EXPERIMENTAL

Investigations were carried out on a corundum material with an aluminium oxide content of about 96% and a chemical composition shown in Table 1. Samples in the form of bars were prepared by pressing /at a pressure of 1400 kG/cm^2/ and fired at 1750^{o}C in a gas furnace. Preparations for microscopic studies were cut out of the samples with an Isomet saw. Polished sections obtained by successive grinding and polishing were investigated with a Jeol J SM-2 scanning microscope and a JXA-3A electron microprobe. For transmission electron microscopy /JEM--120 microscope/ the samples were ground and polished to a thickness of about 100 μm, whereupon they were thinned until perforation was obtained by bilateral bombardment with argon ions at an angle of 30^o in a Commonwealth Scientific Corporation IMMI Model V apparatus operated at an accelerating voltage of 6 kV and a beam current of 100 μA. In the final stage of sample preparation the bombardment was conducted at an angle of 10^o so that the ion beam would have a polishing effect. Due to

Table 1

Initial chemical composition of the material studied

Component	Al_2O_3	SiO_2	CaF_2	MgO	BaF_2	Cr_2O_3
Content /wt.%/	95.93	1.57	0.90	0.60	0.50	0.50

this procedure, samples were obtained with sufficiently large areas transparent to an electron beam of an energy of 120 keV. The thinning time of one samples was about 120 hs. Before the samples was mounted in the electron microscope, its surface was coated with a thin /~ 25 Å/ carbon layer to carry off the electric charge generated at the surface, and to eliminate interferences resulting from the electrostatic interaction of the beam with this charge.

RESULTS AND DISCUSSION

As appears from the observations of the unetched surfaces of polished sections /Phot. 1/, two types of microareas /*B* and *C*/ can be distinguished in the material studied besides aluminium oxide grains and pores. One type is represented by microareas of a prevalently triangular shape and maximum linear dimensions from one to a dozen or so micrometres; the other by irregular polygons of a size approximately equal to that of Al_2O_3 grains. The two types also differ in chemical composition. As is evident from microprobe analysis, type *B* microareas /Phot. 2/ contain all the elements introduced in the technological process, while only aluminium, magnesium, chromium and oxygen /Table 2/ are present in type *C* microareas /Phot. 3/.

Table 2

Mass freaction of elements entering into the composition of the intergranular phase, calculated from relative intensities of the characteristic radiation

Microarea studied	Element						
	Mass fractions /wt.%/						
	Al	O	Mg	Cr	Si	Ca	Ba
Area *B*	11.3	37.6	2.6	2.4	27.0	6.4	4.4
Area *C*	31.4	43.4	17.9	2.6	-	-	-

Mass fractions of the elements occurring in the analysed microareas, calculated from relative intensities of the characteristic radiation, are given in Table 2.

Transmission electron micrographs are shown in photographs 4 and 5. Microdiffraction performed from type *B* microareas /Phot. 6/ indicates that they are amorphous in nature, whereas the patterns obtained from type C areas /Phot. 7/ correspond to a structure of the aluminium-magnesium spinel type. These results have been confirmed by microprobe studies. Discrepancies, amounting to about 17%, have been noted between the values of interplanar spacings obtained by the authors /lower values/ and those given by Mitchell /1979/. Further investigations are required to find the causes of these discrepancies. It seems, however, that the presence of chromium in the structure of spinel phase is responsible for the noted differences.

CONCLUSIONS

From the above studies it appears that the investigated corundum material has aluminium oxide grains as well as an amorphous vitreous phase and crystalline spinel phase containing certain amounts of chromium in its composition.

REFERENCES

BURKE J., 1960 - Grain growth in ceramics. Kinetics of high temperature processes. New York, ed. J. Wiley.

COLE S. S., SOMMER G., 1961 - Glass migration mechanism of ceramic to metal seal adherence. *J. Amer. Ceram. Soc.* 44/6/.

KITAJGORODZKI J., 1959 - Das Glass in der Keramik. *Silikattechnik* 8.

MITCHELL T. E., 1979 - Application of transmission electron microscopy to the study of deformation in ceramic oxides. *J. Amer. Ceram. Soc.* 62/5-6/.

PAMPUCH R., 1962 - Spiekanie krystalicznych proszków. *Zesz. Nauk. AGH* 10.

WŁOSIŃSKI W., 1976 - Zjawiska dyfuzyjne w granicznych warstwach połączeń ceramika-metal w aspekcie optymalizacji technologii. *Praca ONPMP* 11.

Leonard KULIG, Henryk TOMASZEWSKI, Jędrzej TORUŃ

BADANIA MIKROSKOPOWE FAZY MIEDZYZIARNOWEJ TWORZYW KORUNDOWYCH

S t r e s z c z e n i e

Wybrane tworzywo korundowe badano metodami TEM, SEM i EPMA. Stwierdzono obecność dwóch rodzajów fazy międzyziarnowej. Obok mikroobszarów fazy szklistej zaobserwowano mikroobszary spinelu glinowo-magnezowego.

OBJAŚNIENIE FOTOGRAFII

Fot. 1a, b. Powierzchnia nietrawionego zgładu badanego tworzywa korundowego. Zdjęcie wykonane metodą elektronów wtórnych /SEM/

A - ziarna tlenku glinowego, *B* - mikroobszary fazy bezpostaciowej, *C* - mikroobszary fazy spinelowej

Fot. 2. Rozkłady natężenia promieniowania charakterystycznego w mikroobszarach fazy typu *B* /fazy szklistej/

a - obraz topograficzny

Fot. 3. Rozkłady natężenia promieniowania charakterystycznego pierwiastków w mikroobszarze fazy typu *C* /fazy spinelowej/

a - obraz topograficzny

Fot. 4. Obraz mikrostruktury badanego tworzywa wykonany metodą wiązki przechodzącej /TEM/

A - ziarna tlenku glinowego, *B* - mikroobszar fazy bezpostaciowej

Fot. 5. Obraz mikroskopowy mikroobszaru fazy spinelowej /faza *C*/ z układem dyslokacji /TEM/

Fot. 6. Obraz dyfrakcyjny mikroobszaru fazy szklistej /faza *B*/

Fot. 7. Obraz dyfrakcyjny mikroobszaru fazy spinelowej z wyznaczonymi wskaźnikami Millera

Леонард КУЛИГ, Хэнрык ТОМАШЕВСКИ, Енджей ТОРУНЬ

МИКРОСКОПИЧЕСКИЕ ИССЛЕДОВАНИЯ МЕЖЗЕРНОВОЙ ФАЗЫ КОРУНДОВЫХ МАТЕРИАЛОВ

Р е з ю м е

Избранные корундовые материалы изучались TEM, SEM и EPMA методами. Обнаружено присутствие двух видов межзерновой фазы. Кроме микроучастков стекловидной фазы, наблюдались микроучастки алюминиуво-магниевой шпинели.

ОБЪЯСНЕНИЯ К ФОТОГРАФИЯМ

Фото 1а, b. Поверхность нетравленного аншлифа изучаемого корундового материала. Снимок сделан методом вторичных электронов /МЭВ/

А — зерна окиси алюминия, В — микроучастки аморфной фазы, С — микроучастки шпинелевой фазы

Фото 2. Распределение интенсивности излучения, характерного в микроучастках фазы типа В /стекловидной фазы/

a — топографическая картина

Фото 3. Распределение интенсивности характерного излучения в микроучастках фазы типа *C* /шпинелевой фазы/

a — топографическая картина

Фото 4. Образ микроструктуры изучаемого материала, полученный методом проходящего пучка /МПП/

A — зерна окиси алюминия, *B* — микроучасток аморфной фазы

Фото 5. Микроскопическая картина микроучастка шпинелевой фазы /фаза *C*/ с системой дислокации /МПП/

Фото 6. Дифракционная картина микроучастка стекловидной фазы /фаза *B*/

Фото 7. Дифракционная картина микроучастка шпинелевой фазы *C* определенными показателями Миллера

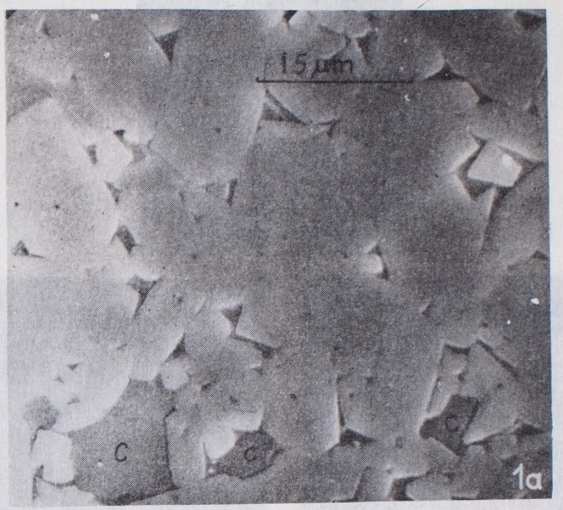

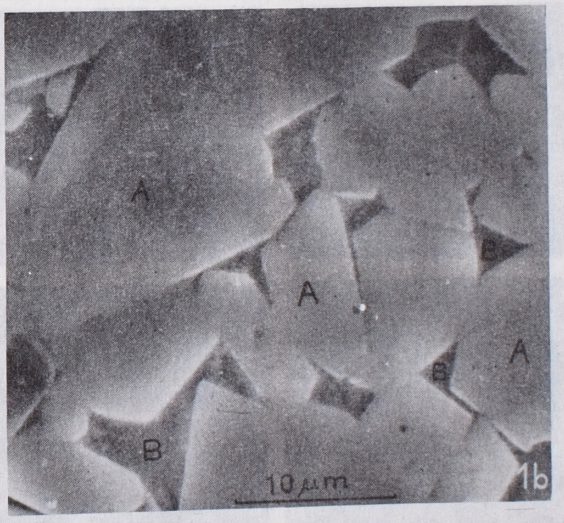

Phot. 1a, b. Unetched polished surface of corundum material. Images are taken by secondary electron method. SEM

A - Aluminium oxide grains, *B* - Microareas of amorphous phase, *C* - Microareas of spinel phase

Leonard KULIG, Henryk TOMASZEWSKI, Jędrzej TORUŃ - Microscopic studies of the intergranular phase in corundum materials

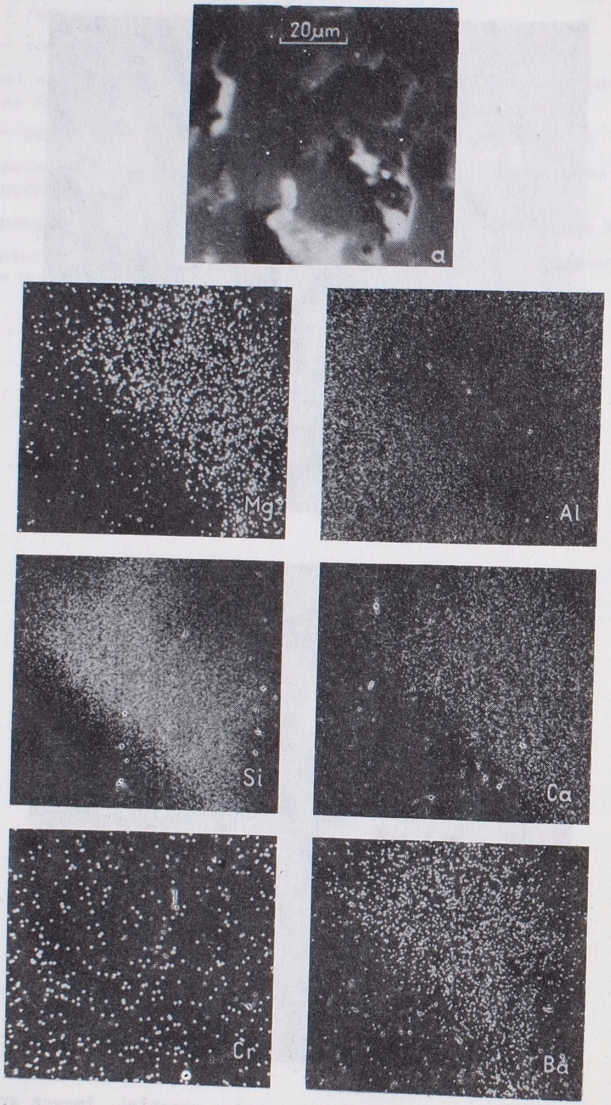

Phot. 2. Electron-probe microanalysis. X-ray microprobe images in type *B* microareas /vitreous phase/

a - topography; Mg, Al, Si, Ca, Cr, Ba - distribution of: magnesium, aluminium, silica, calcium, chromium, barium

Leonard KULIG, Henryk TOMASZEWSKI, Jędrzej TORUŃ - Microscopic studies of the intergranular phase in corundum materials

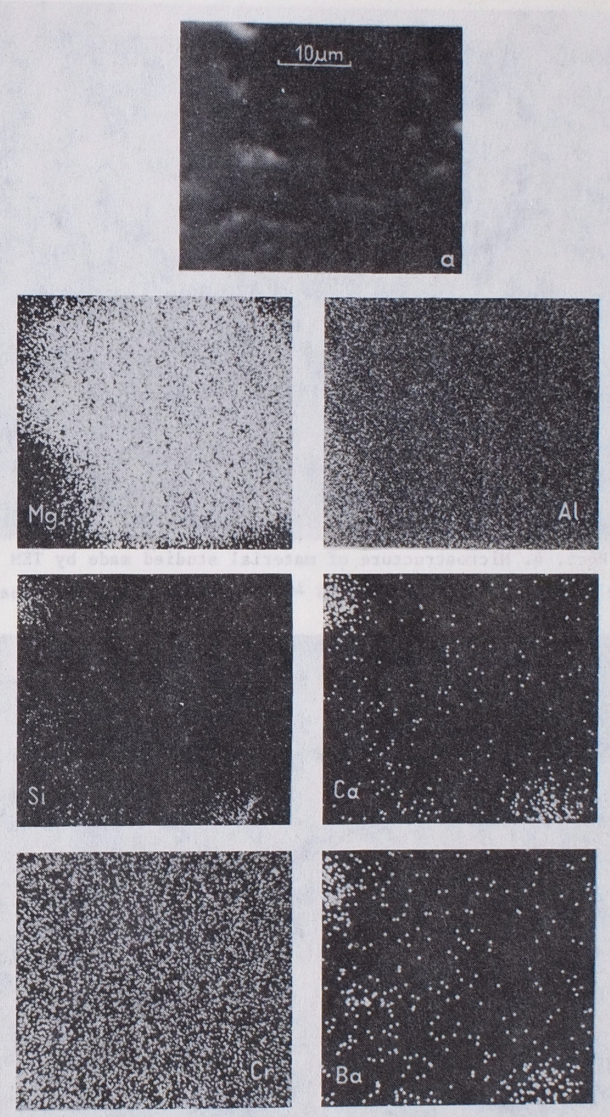

Phot. 3. Electron-probe microanalysis. X-ray microprobe images in type *C* microarea /spinel phase/

a - topography; Mg, Al, Si, Ca, Cr, Ba - distribution of: magnesium, aluminium, silica, calcium, chromium, barium

Leonard KULIG, Henryk TOMASZEWSKI, Jędrzej TORUŃ - Microscopic studies of the intergranular phase in corundum materials

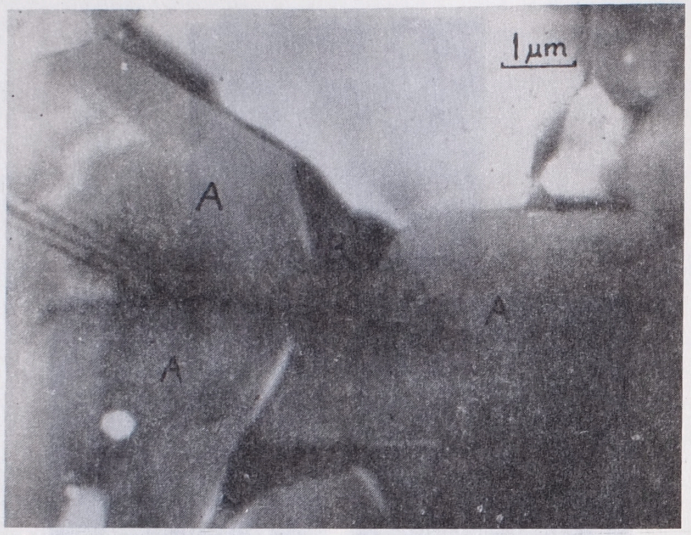

Phot. 4. Microstructure of material studied made by TEM
A - aluminium oxide grains, *B* - microarea of amorphous phase

Phot. 5. Electron micrograph performed from spinel phase */C/* microarea with dislocation system /TEM/

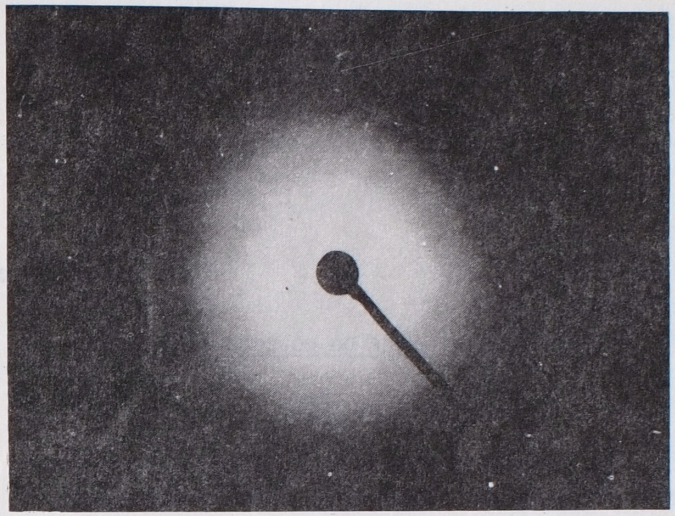

Phot. 6. Electron diffraction of type *B* microarea /vitreous phase/

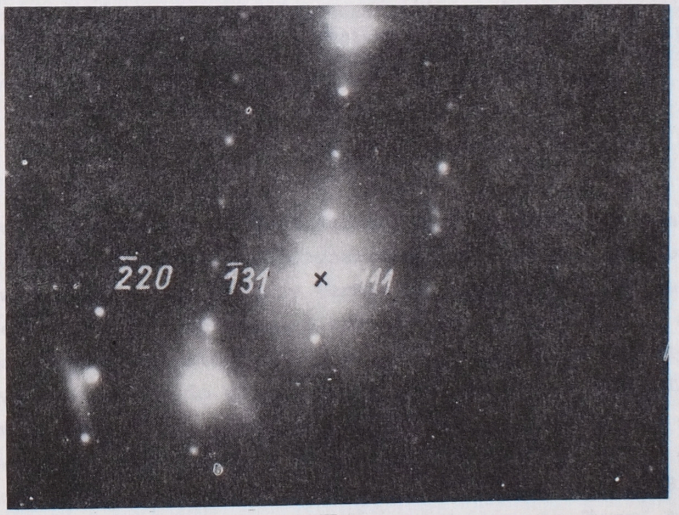

Phot. 7. Electron diffraction of spinel phase microarea with *hkl* Miller's indices